

## Supporting Information

### **2D Hetero-nanostructural Reduced-CuNiFe-Oxides with Self-produced H<sub>2</sub>O<sub>2</sub> Fenton-like Photocatalysis for Tetracycline Degradation**

Lin Fu<sup>a,‡</sup>, Dandan Wu<sup>b,‡</sup>, Ming Wen<sup>a,\*</sup>, Yuanzheng Zhu<sup>c</sup>, Qingsheng Wu<sup>a</sup>, Tao Zhou<sup>a</sup>, Yongqing Fu<sup>d</sup>

<sup>a</sup> *School of Chemical Science and Engineering, School of Environmental Science and Engineering, The State Key Laboratory of Pollution Control and Resource Reuse, Shanghai Key Laboratory of Chemical Assessment and Sustainability, Tongji University, Shanghai 200092, P. R. China.*

<sup>b</sup> *School of Materials Science and Engineering, Shanghai Institute of Technology, Shanghai 201418, P. R. China*

<sup>c</sup> *School of Materials and Chemistry, University of Shanghai for Science and Technology, Shanghai, 200093, P. R. China*

<sup>d</sup> *Faculty of Engineering and Environment, Northumbria University, Newcastle upon Tyne NE99, UK*

\* *Corresponding author. E-mail: m\_wen@tongji.edu.cn (M. Wen).*

‡ *These authors contributed equally to this work.*

## S1 Materials and reagent

The following chemicals were supplied by Sinopharm Chemical Reagent Co., Ltd. (China) including copper nitrate trihydrate ( $\text{Cu}(\text{NO}_3)_2 \cdot 3\text{H}_2\text{O}$ ,  $\geq 99.0\%$ ), iron nitrate nonahydrate ( $\text{Fe}(\text{NO}_3)_3 \cdot 9\text{H}_2\text{O}$ ,  $\geq 99.99\%$ ), sodium hydroxide (NaOH, 90%), nickel nitrate hexahydrate ( $\text{Ni}(\text{NO}_3)_2 \cdot 6\text{H}_2\text{O}$ ,  $\geq 98.0\%$ ), urea ( $\text{H}_2\text{NCONH}_2$ , AR), ethylene glycol ( $(\text{CH}_2\text{OH})_2$ , AR), hydrochloric acid (HCl, AR), sodium bicarbonate ( $\text{NaHCO}_3$ ,  $\geq 99.8\%$ ), ethanol ( $\text{CH}_3\text{CH}_2\text{OH}$ ,  $\geq 99.7\%$ ), triethanolamine (TEA,  $\text{C}_6\text{H}_{15}\text{NO}_3$ , AR), tert-butanol (TBA,  $\text{C}_4\text{H}_{10}\text{O}$ , AR), p-benzoquinone (BQ,  $\text{C}_6\text{H}_4\text{O}_2$ ,  $\geq 97.0\%$ ), furfuryl alcohol (FFA,  $\text{C}_5\text{H}_6\text{O}_2$ ,  $\geq 97.0\%$ ). Catalase (bovine liver BR, 2000-5000  $\text{u} \cdot \text{mg}^{-1}$ ) was obtained from Shanghai Yuanye Biotechnology Co., Ltd. Escherichia coli (*E. coli*) was obtained from Shanghai Benoy Biological. Tetracycline (TC,  $\text{C}_{22}\text{H}_{24}\text{N}_2\text{O}_8$ ,  $\geq 98.0\%$ ), chlortetracycline (CTC,  $\text{C}_{22}\text{H}_{23}\text{ClN}_2\text{O}_8$ ,  $\geq 95.0\%$ ), and oxytetracycline (OTC,  $\text{C}_{22}\text{H}_{25}\text{ClN}_2\text{O}_9$ ,  $\geq 99.0\%$ ) were obtained from Solarbio (Beijing). All the reagents in the experiment were of analytical grade, without further purified.

## S2 Bacterial culture experiments

The bacteria strains were cultured in nutrient broth  $10 \text{ g} \cdot \text{L}^{-1}$  peptone,  $5 \text{ g} \cdot \text{L}^{-1}$  yeast extract,  $10 \text{ g} \cdot \text{L}^{-1}$  NaCl, pH = 7.2, and then added to  $500 \mu\text{g} \cdot \text{L}^{-1}$  TC solution after degradation under light irradiation or dark in an incubator, for overnight at  $37 \pm 1 \text{ }^\circ\text{C}$ . The prepared 30 mL bacteria were centrifuged and washed 3 times with 0.9% NaCl, and diluted into 30 mL with 0.9% NaCl. The bacterial concentration was then determined by the plate method. Before carrying out the bacterial culture experiment, the stains was cultured and washed according to the above method, and then diluted with 0.9% NaCl to the designed concentration, which is the stock bacteria solution. The stock bacteria solution was used within 3 hrs, and its concentration was measured as the initial bacterial concentration. The TC solutions after Fenton-like photocatalysis for 0 hr, 4 hrs, 12 hrs were added into the above system, and the bacterial concentrations in the different systems were tested using the same method as described above. The bacteria used in this experiment was *E. coli*.

**Table S1.** Surface areas, total pore volumes, and average pore diameters data of the prepared materials obtained using BET method.

Materials	BET surface area (m <sup>2</sup> ·g <sup>-1</sup> )	Total Pore volume (cm <sup>3</sup> ·g <sup>-1</sup> )	Average pore Diameter (nm)
re-CuNiFe-MMOs	126	0.32	24
re-CuFe-MMOs	47	0.0033	5.72
re-CuNi-MMOs	114	0.25	16
re-FeNi-MMOs	118	0.23	11

**Table S2.** Reaction rate constants in different cycles of re-CuNiFe-MMOs nanocomposite as catalysts.

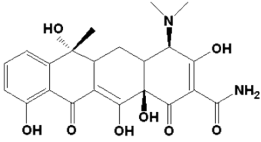
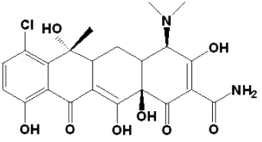
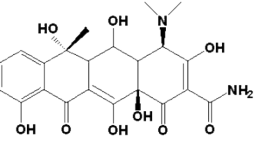
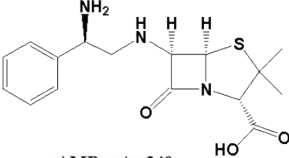
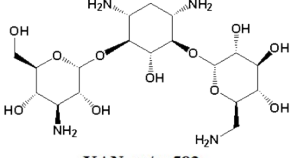
No. of cycles	re-CuNiFe-MMOs nanocomposite reaction rate constants $k$ (min <sup>-1</sup> )
1	1.65
2	1.53
3	1.44
4	1.37
5	1.31
6	1.22
7	1.14
8	1.06
9	1.00
10	0.93
11	0.83
12	0.70

The results of degradation data indicate that the reaction kinetics of antibiotic degradation satisfies the pseudo-first-order kinetic model, and therefore, the kinetic parameters were calculated according to the following equations:

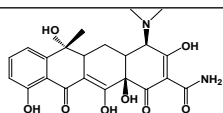
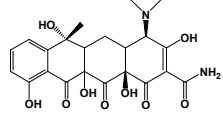
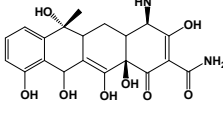
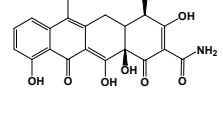
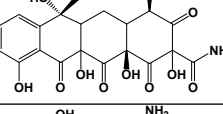
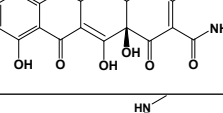
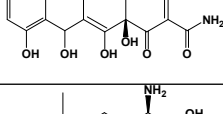
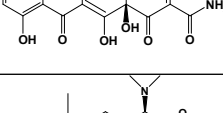
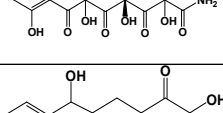
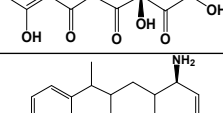
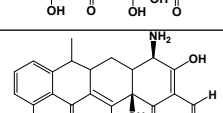

$$\frac{dc}{dt} = -k \cdot [c]$$
$$\ln \frac{C_t}{C_0} = -k \cdot t$$

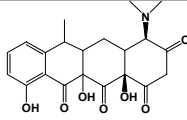
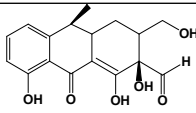
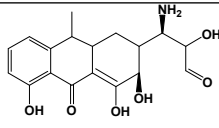
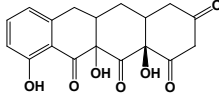
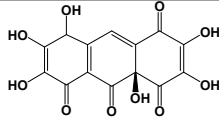
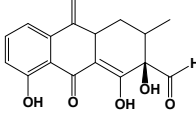
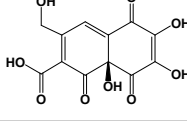
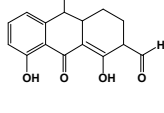
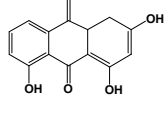
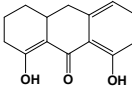
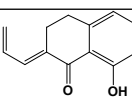
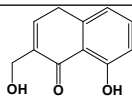
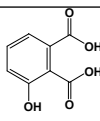
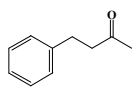
where  $t$  is the reaction time,  $C_0$  is the initial antibiotic concentration,  $C_t$  is the antibiotic concentration at reaction time  $t$ , and  $k$  is the rate constant.

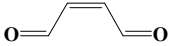
**Table S3.** A List of Molecular Structure Formulas

	Tetracycline (TC)	Chlortetracycline (CTC)	Oxytetracycline (OTC)
<b>Tetracycline antibiotics</b>	 <p>TC <math>m/z=445</math></p>	 <p>CTC <math>m/z=479</math></p>	 <p>OTC <math>m/z=461</math></p>
<b>Non-tetracycline antibiotics</b>	<b>Ampicillin (AMP)</b>  <p>AMP <math>m/z=349</math></p>	<b>Kanamycin (KAN)</b>  <p>KAN <math>m/z=583</math></p>	

**Table S4.** Potential intermediates detected during TC degradation in re-CuNiFe-MMOs system under visible light irradiation.

Number	m/z	Molecular formula	Molecular structural formula
TC	445	$C_{22}H_{24}O_8N_2$	
TC1	461	$C_{22}H_{24}O_9N_2$	
TC2	431	$C_{21}H_{22}O_8N_2$	
TC3	427	$C_{22}H_{22}O_7N_2$	
TC4	477	$C_{22}H_{24}O_{10}N_2$	
TC5	403	$C_{19}H_{18}O_8N_2$	
TC6	417	$C_{20}H_{20}O_8N_2$	
TC7	399	$C_{20}H_{18}O_7N_2$	
TC8	459	$C_{22}H_{24}O_9N_2$	
TC9	376	$C_{20}H_{17}O_7N$	
TC10	352	$C_{20}H_{17}O_5N$	
TC11	384	$C_{20}H_{17}O_7N$	

TC12	400	$C_{21}H_{21}O_7N$	
Number	m/z	Molecular formula	Molecular structural formula
TC13	318	$C_{17}H_{16}O_6N$	
TC14	346	$C_{18}H_9O_6N$	
TC15	343	$C_{18}H_{14}O_7$	
TC16	337	$C_{14}H_8O_{10}$	
TC17	301	$C_{17}H_{17}O_5$	
TC18	297	$C_{12}H_8O_9$	
TC19	274	$C_{15}H_{14}O_5$	
TC20	256	$C_{15}H_{12}O_4$	
TC21	230	$C_{14}H_{14}O_3$	
TC22	200	$C_{13}H_{12}O_2$	
TC23	189	$C_{11}H_9O_3$	
TC24	183	$C_8H_6O_5$	
TC25	148	$C_{10}H_{13}O$	

TC26	84	$C_4H_4O_2$	
------	----	-------------	---

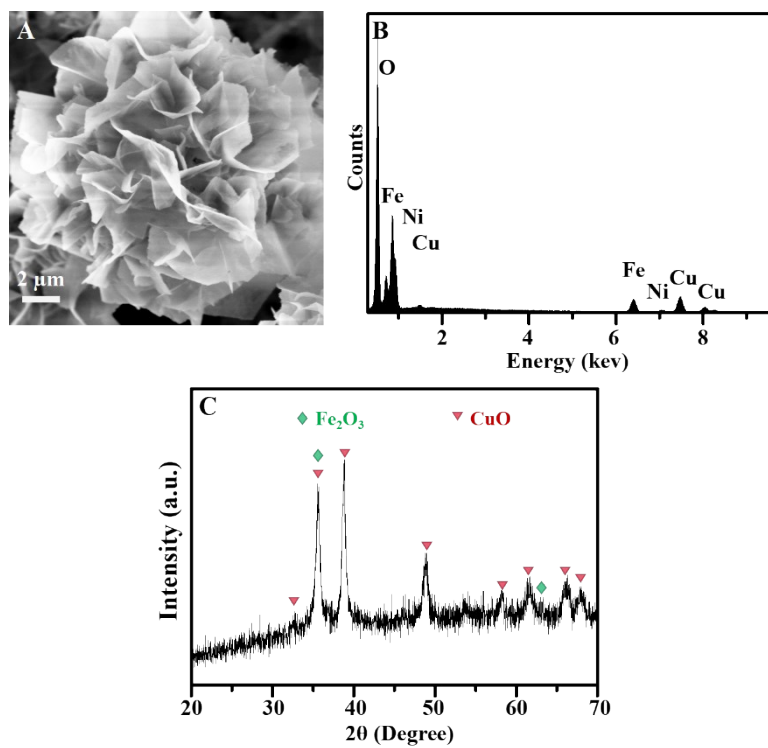


**Fig. S1.** CuNiFe-MMOs precursor characterization results: (A) SEM image, (B) EDS, (C) XRD pattern.

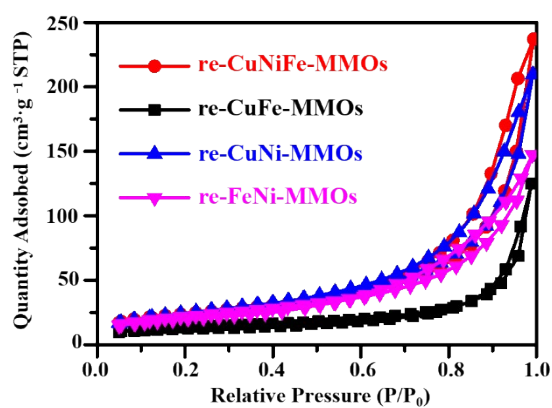


**Fig. S2.** N<sub>2</sub> adsorption-desorption isotherms of the prepared catalysts.

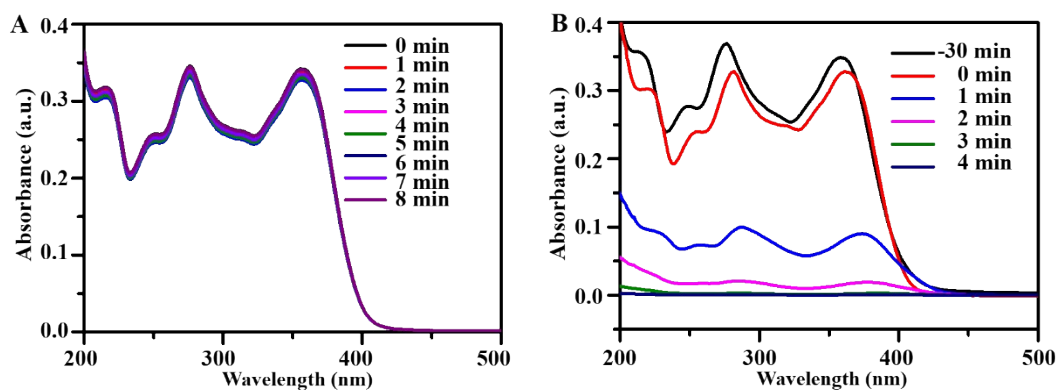


**Fig. S3.** UV-vis spectra of TC degradation catalyzed by re-CuNiFe-MMOs at different conditions: (A) blank experiment without catalyst; (B) visible light irradiation.

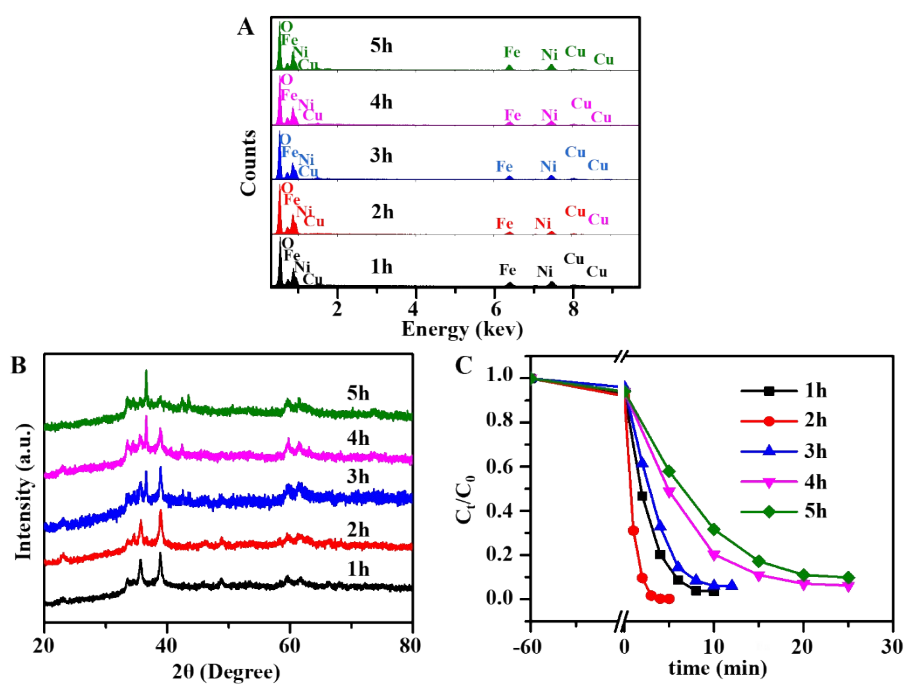


**Fig. S4.** Characterization results of re-CuNiFe-MMOs synthesized in different reduction time: (A) EDS, (B) XRD patterns, and (C) catalytic behavior of TC degradation. (re-CuNiFe-MMOs obtained at reduction time of 2 hrs gets the best performance for the Fenton-like photocatalytic degradation of TC).



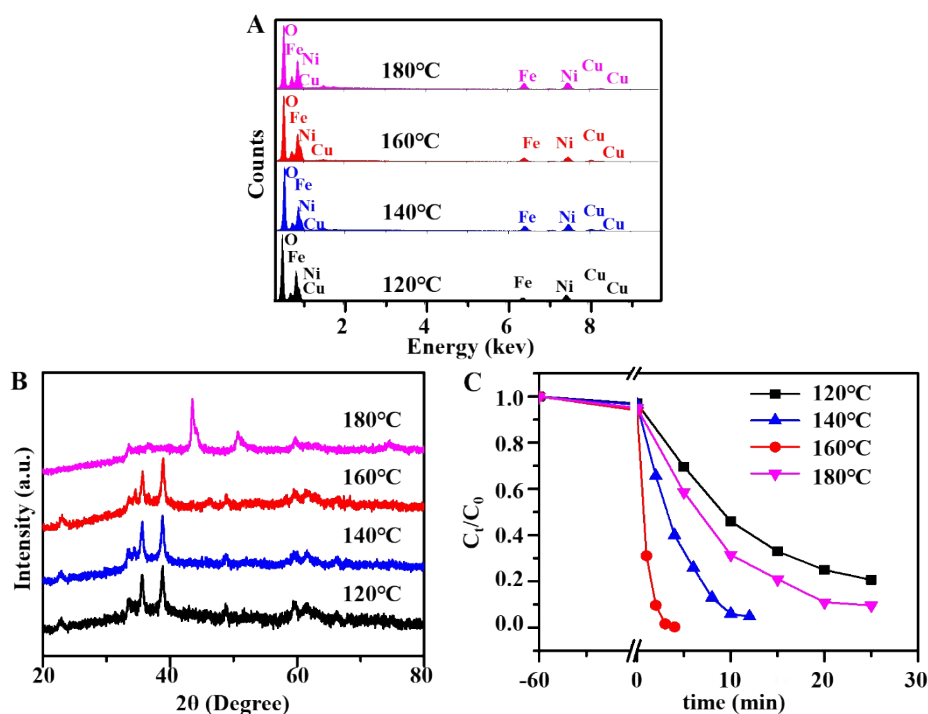


**Fig. S5.** Characterization results of re-CuNiFe-MMOs synthesized at different reduction temperatures: (A) EDS, (B) XRD patterns, and (C) catalytic behavior of TC degradation.

(re-CuNiFe-MMOs obtained at reduction temperature of 160 °C gains the top performance for the Fenton-like photocatalytic degradation of TC.)

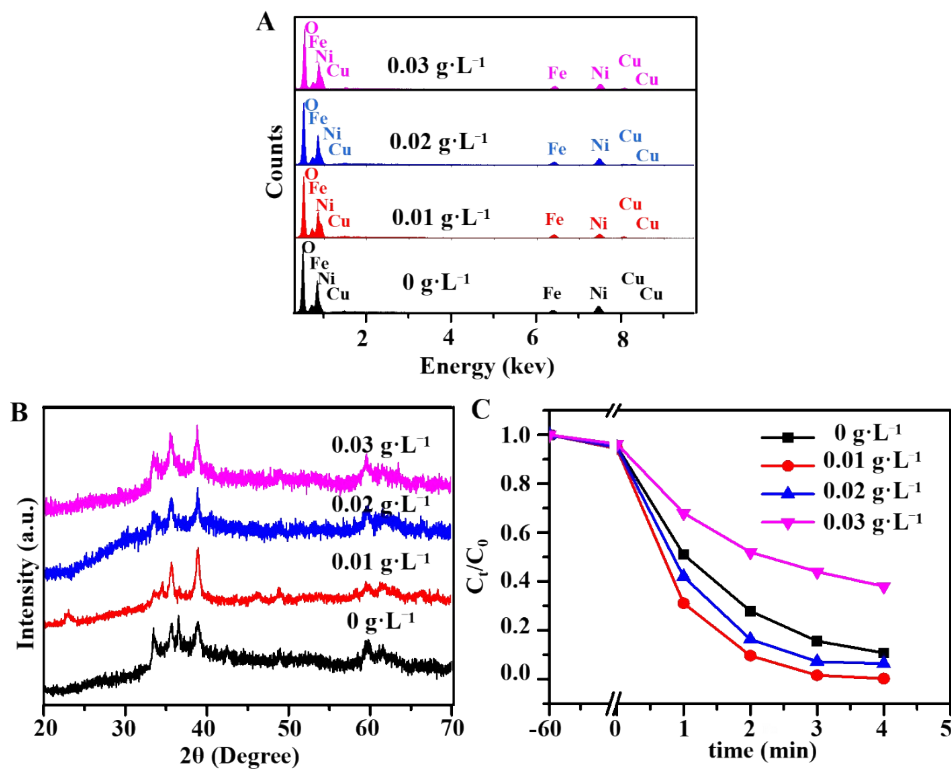


**Fig. S6.** Characterization results of re-CuNiFe-MMOs synthesized in different concentrations of NaHCO<sub>3</sub>: (A) EDS, (B) XRD patterns, and (C) catalytic behavior of TC degradation.

(re-CuNiFe-MMOs obtained at 0.01 g·L<sup>-1</sup> NaHCO<sub>3</sub> wins the best performance for the Fenton-like photocatalytic degradation of TC).

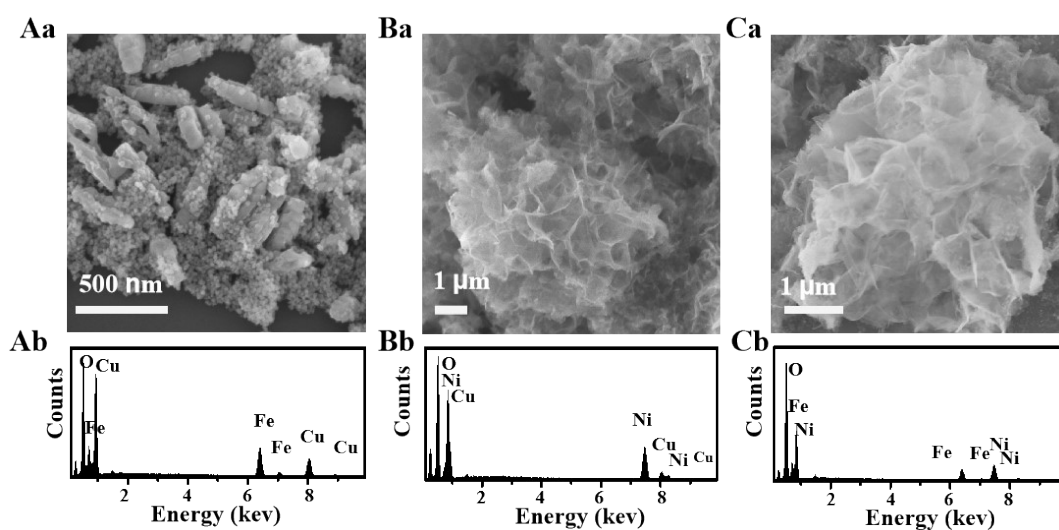


**Fig. S7.** SEM (a) and EDS (b) of the prepared samples: (A) re-CuFe-MMOs, (B) re-CuNi-MMOs, and (C) re-FeNi-MMOs.

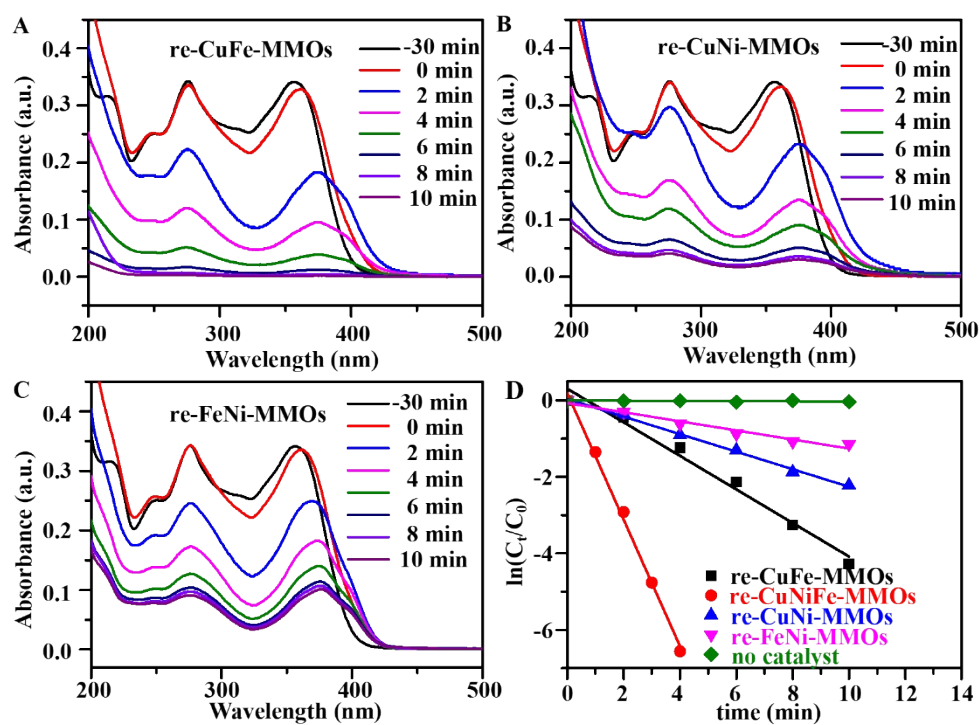


**Fig. S8.** TC degradation results catalyzed by the prepared catalysts under visible-light irradiation: (A-C) UV-vis spectra; (D) The corresponding pseudo-first-order kinetic model. The TC degradation rates using re-CuNiFe-MMOs, re-CuFe-MMOs, re-CuNi-MMOs, and re-FeNi-MMOs are 99.9% ( $K=1.65 \text{ min}^{-1}$ ), 72.1% ( $K=0.44 \text{ min}^{-1}$ ), 60.6% ( $K=0.23 \text{ min}^{-1}$ ) and 46.5% ( $K=0.12 \text{ min}^{-1}$ ) within a 4 min period, respectively.

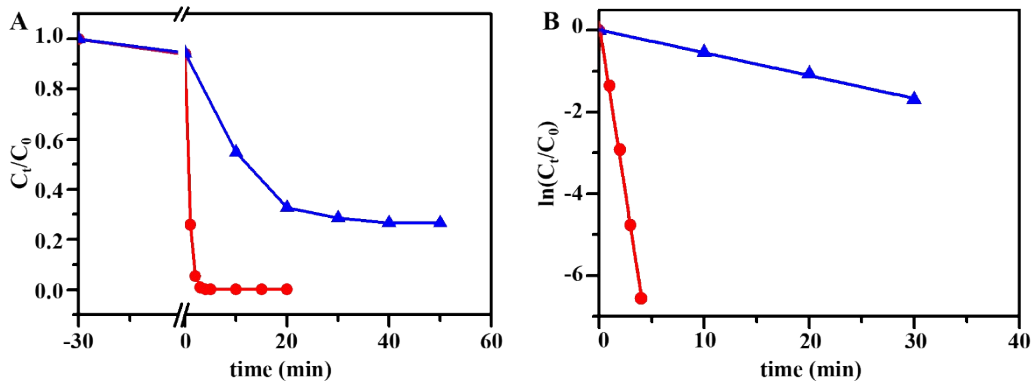


**Fig. S9.** (A) Profiles of TC degradation catalyzed by re-CuNiFe-MMOs (red) and CuNiFe-MMOs (blue) under visible-light irradiation; (B) their corresponding pseudo-first-order kinetic models.

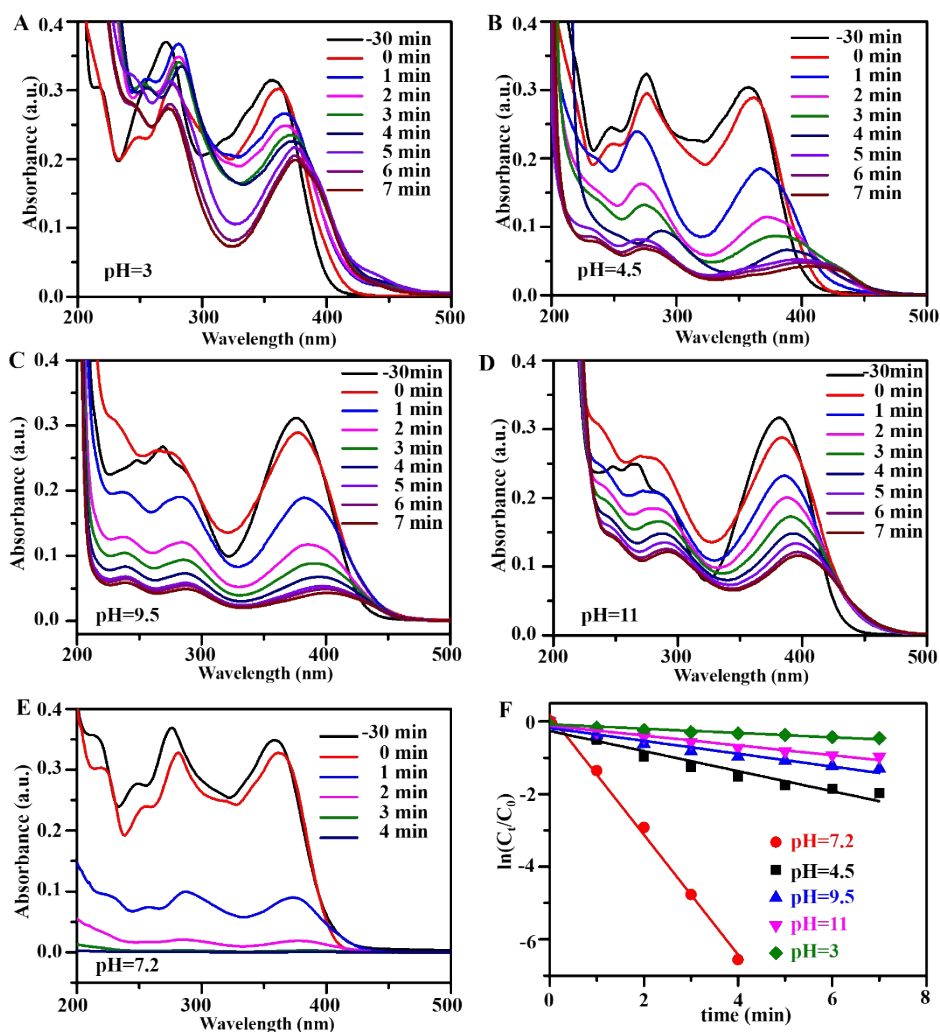


**Fig. S10.** TC degradation catalyzed by re-CuNiFe-MMOs in different pH under visible-light irradiation: (A-E) UV-vis spectra; (F) The corresponding pseudo-first-order kinetic models.

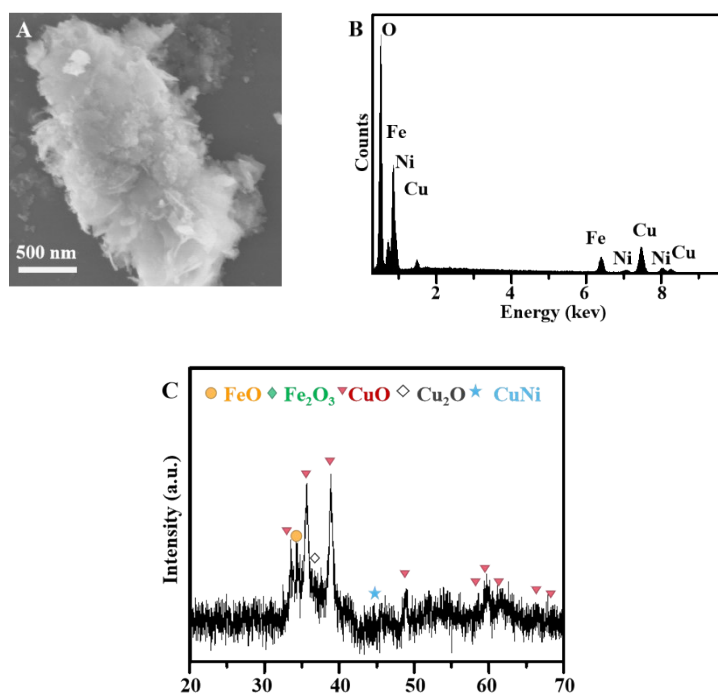


**Fig. S11.** Characterization results of re-CuNiFe-MMOs obtained by H<sub>2</sub> reduction: (A) SEM, (B) EDS, (C) XRD.

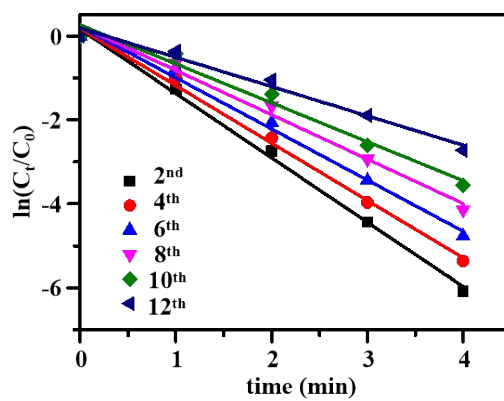


**Fig. S12.** The linear plots of  $\ln(C_t/C_0)$  versus time of the 2<sup>nd</sup>, 4<sup>th</sup>, 6<sup>th</sup>, 8<sup>th</sup>, 10<sup>th</sup>, and 12<sup>th</sup> cycles in TC degradation cycling test catalyzed by re-CuNiFe-MMOs.

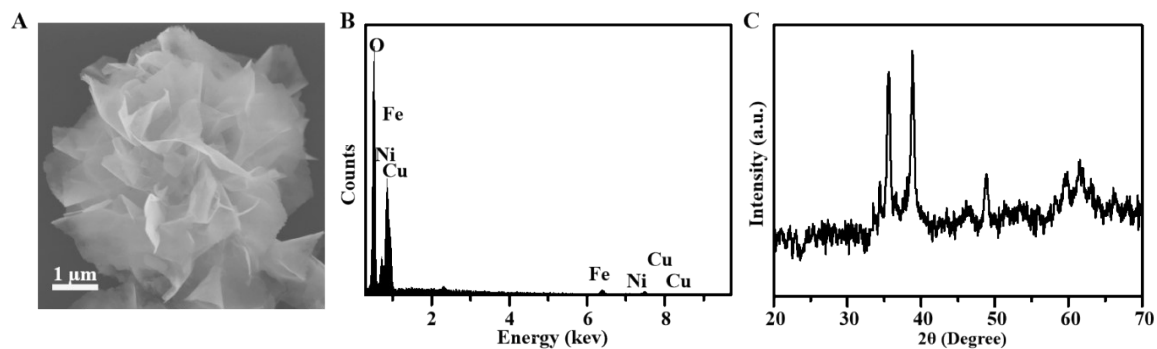


**Fig. S13.** SEM (A), EDS (B), and XRD (C) pattern over re-CuNiFe-MMOs after TC degradation for twelve consecutive recycling experiments.

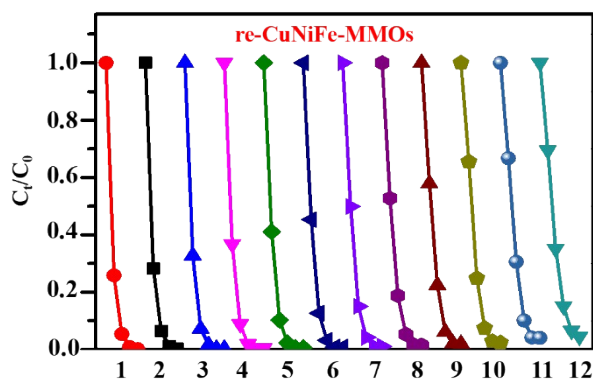


**Fig. S14.** TC degradation cycling test catalyzed by re-CuNiFe-MMOs.

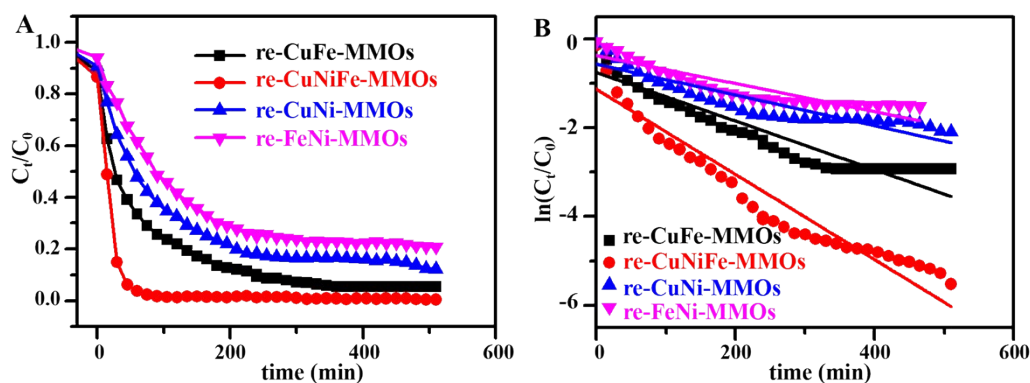


**Fig. S15.** (A) Profiles of TC ( $50\text{mg}\cdot\text{L}^{-1}$ ) degradation and (B) their corresponding pseudo-first-order kinetic model catalyzed by the prepared photocatalysts.

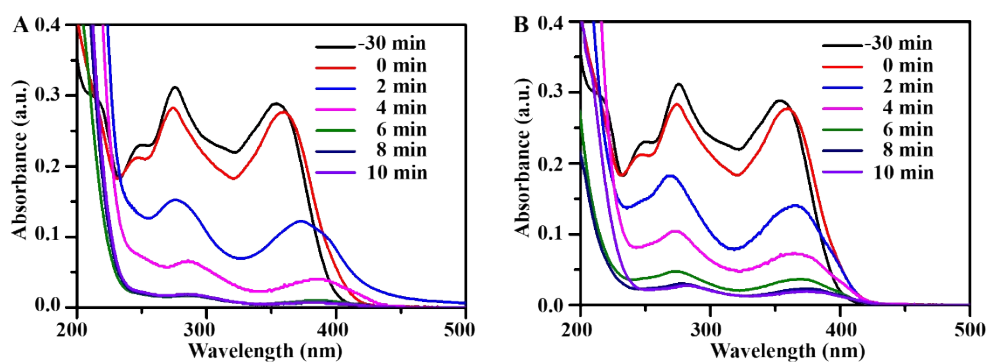


**Fig. S16.** UV-vis spectra of TCs at different degradation periods: (A) CTC, and (B) OTC by using re-CuNiFe-MMOs catalyst under visible light irradiation.

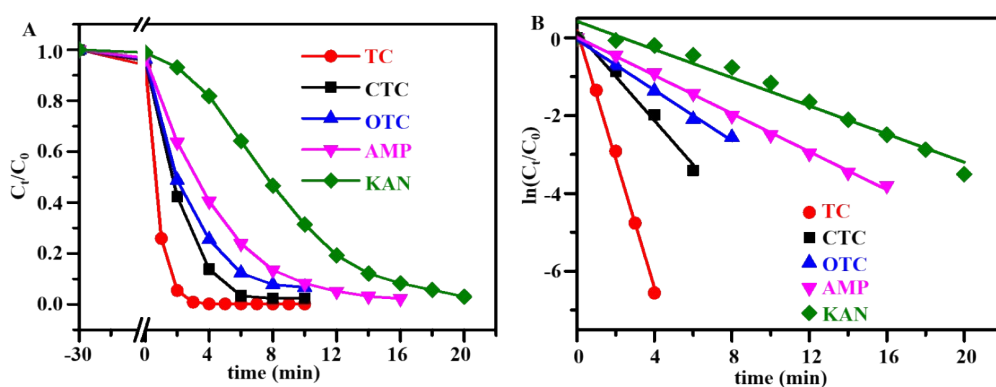


**Fig.S17.** (A) Profiles of TC degradation with (B) corresponding pseudo-first-order kinetic models over the prepared antibiotics. (Operating parameters: 30 min adsorption equilibrium under anaerobic dark condition,  $0.25\text{ g}\cdot\text{L}^{-1}$  catalyst,  $10\text{ mg}\cdot\text{L}^{-1}$  antibiotics,  $25\text{ }^\circ\text{C}$ , pH 7.2).

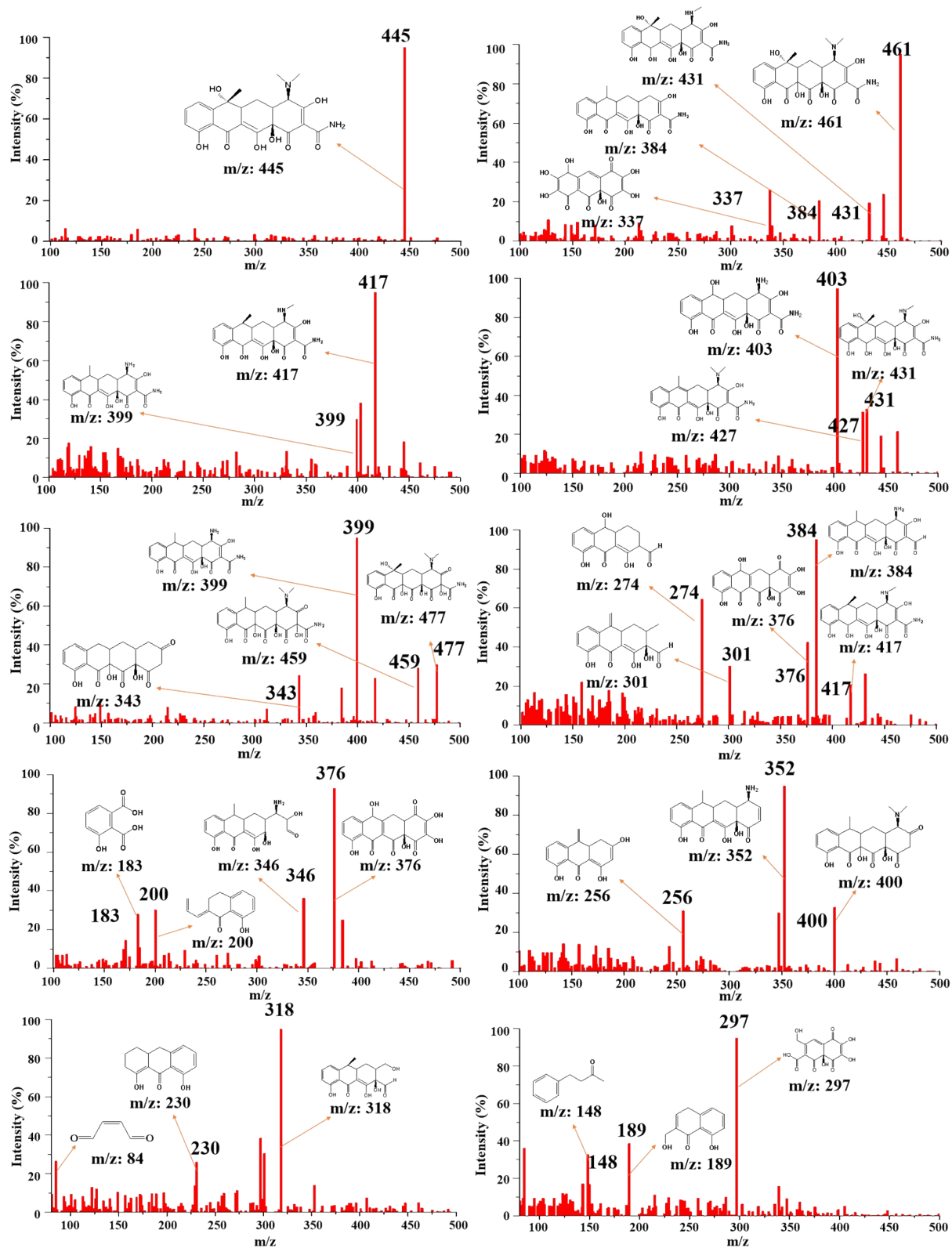


**Fig. S18.** LC-MS spectra of intermediates in TC degradation in re-CuNiFe-MMOs system.

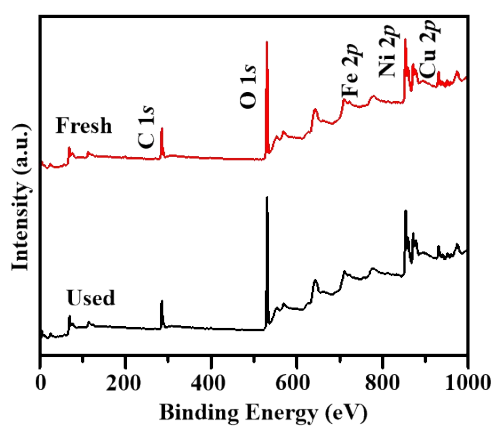


Fig. S19. XPS survey spectra of fresh and used re-CuNiFe-MMOs catalysts.

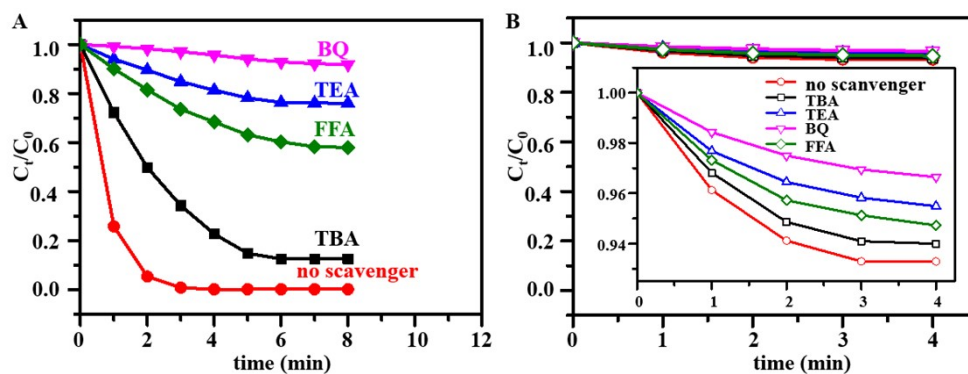
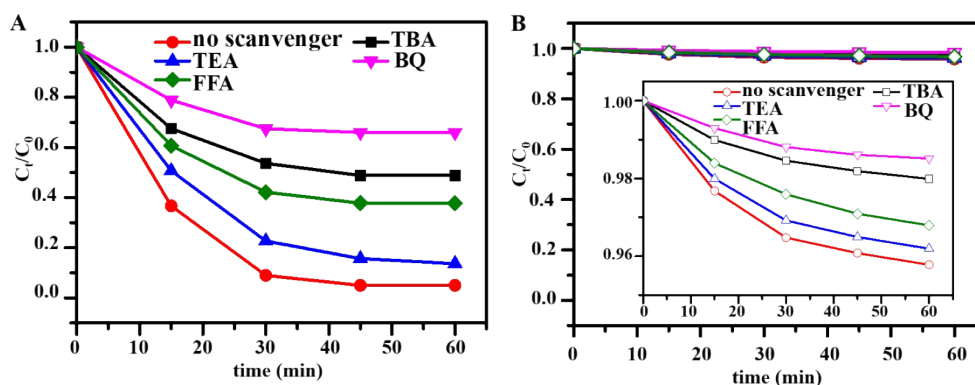


Fig. S20. Active species capture experiments for the TC degradation catalyzed by re-CuNiFe-MMOs at conditions: (A) aerobic under visible light, (B) anaerobic under visible light.





**Fig. S21.** Active species capture experiments for the TC degradation catalyzed by re-CuNiFe-MMOs at conditions: (A) aerobic under dark, (B) anaerobic under dark.

As shown in Fig. S21A, the degradation rate of TC is reached by 95.0 % within 45 min under the dark aerobic conditions. TBA, FFA, TEA and BQ was added to respectively correspond quench the  $\cdot\text{OH}$ ,  $^1\text{O}_2$ ,  $\text{h}^+$  and  $\cdot\text{O}_2^-$  generated during the catalytic reaction. The degradation rates decrease from 95.0% to 86.3%, 51.2%, 62.2% and 34.0%, respectively, indicating that  $\cdot\text{O}_2^-$  is the main active species of under dark aerobic conditions. Whereas, in the dark anaerobic, the degradation rate was greatly inhibited in 4.22%, much less than that under dark aerobic conditions (Fig. S21B). And the degradation rate decreases from 4.2% to 2.0%, 3.8%, 3.2% and 1.5% after adding TBA, FFA, TEA and BQ, respectively. It confirmed that  $\cdot\text{O}_2^-$  is the main active species to degrade TC under dark aerobic conditions.

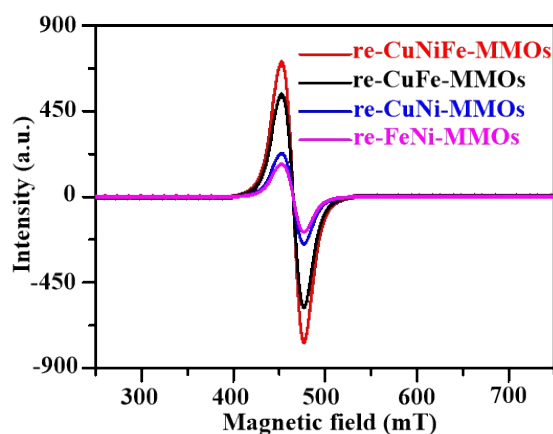


**Fig. S22.** EPR patterns of defects for different samples: (a) re-CuNiFe-MMOs; (b) re-CuFe-MMOs; (c) re-CuNi-MMOs; (d) re-FeNi-MMOs.

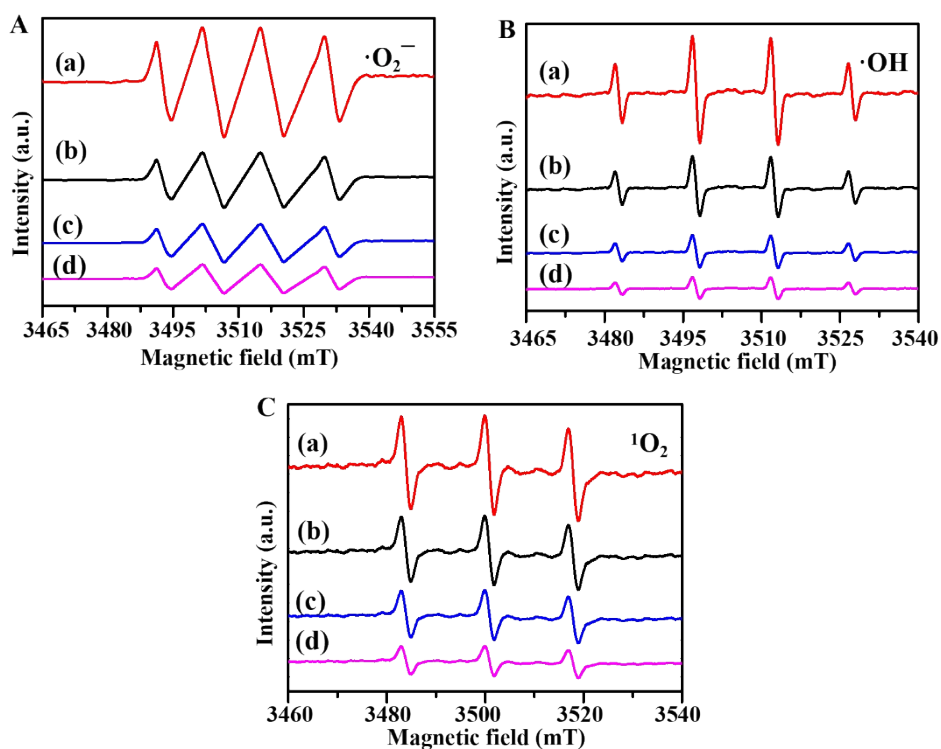


**Fig. S23.** EPR spectra of (A)  $\cdot\text{O}_2^-$ , (B)  $\cdot\text{OH}$ , and (C)  $^1\text{O}_2$  by using the prepared catalysts. ((a) re-CuNiFe-MMOs, (b) re-CuFe-MMOs, (c) re-CuNi-MMOs, (d) re-FeNi-MMOs). (Operating parameters:  $0.25 \text{ g}\cdot\text{L}^{-1}$  catalyst,  $10 \text{ mg}\cdot\text{L}^{-1}$  TC, pH of 7.2)

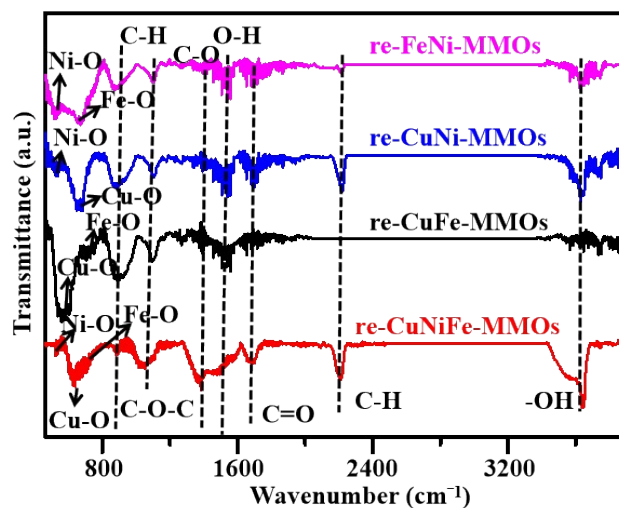


**Fig. S24.** FT-IR spectra of the prepared samples: (a) re-CuNiFe-MMOs; (b) re-CuFe-MMOs; (c) re-CuNi-MMOs; (d) re-FeNi-MMOs.